DEM simulation of particles of complex shapes using the multisphere method: application for additive manufacturing

Eric J. R. Parteli

Institute for Multiscale Simulation, Universität Erlangen-Nürnberg, Nägelsbachstraße 49b, 91052, Erlangen, Germany

Abstract. Additive manufacturing constitutes a promising production technology with potential application in a broad range of industrial areas. In this type of manufacturing process, objects are created from powder particles by adding layers of material upon one another through selectively melting particles from the powder bed. However, understanding the mechanical behavior of the powder during manufacturing as a function of material properties and particle shape is an essential pre-requisite for optimizing the production process. Here we develop a numerical tool for modeling the dynamics of powder particles during additive manufacturing based on force-based simulations by means of the Discrete Element Method (DEM). An existing DEM software (LIGGGHTS) is extended in order to study the transport of powder particles of complex geometric shapes through accounting for the boundary conditions inherent to the manufacturing process.

Keywords: DEM simulation, granular materials, multisphere method, additive manufacturing
PACS: 45.70.-n, 89.20.Bb

INTRODUCTION

Additive manufacturing can provide substantial benefits for part production in a wide range of industrial areas compared to conventional machining [1]. By selectively melting layers of powder particles (e.g. of metallic [2, 3] or thermoplastic materials [4, 5]), parts of almost arbitrarily complex geometries can be efficiently built directly from a three-dimensional (CAD) model. However, important open issues remain to be addressed in order to make this young technology applicable for large-scale production [1]. In particular, understanding the mechanical behaviour of the powder particles during the manufacturing process is essential for developing optimization routes towards improved part quality and shorter production time [4, 6]. Numerical simulations by means of the Discrete Element Method (DEM) [7, 8, 9, 10, 11, 12, 13] can provide an useful tool for modeling particle dynamics as a function of material properties and particle shape.

In the present work, we develop a numerical tool, based on an existing DEM solver [14], for modeling the dynamics of geometrically complex particles subjected to dynamic boundary conditions inherent to additive manufacturing. The purpose of this paper is to present a description of this numerical tool, thereby highlighting the main modifications made in the original DEM for modeling powder particles of complex shapes. Our simulations incorporate an improved model for the normal collisional forces between particles [15], as well as an analytical calculation of the moment of inertia of complex particles built with the multisphere method. In order to illustrate our model, we present snapshots of a simulation of the transport of complex particles in a device mimicking the one used in additive manufacturing.

MODEL FOR THE POWDER PARTICLES

In our simulations, powder particles of complex shapes are modeled as sphere clumps (rigid bodies) using the multisphere method. Constituent spheres of a rigid body interact with spheres belonging to neighbouring particles through viscoelastic forces as we describe below.

Normal forces — During the collision, both particles undergo a small deformation, ξ, along the axis connecting their centers. The normal force on each particle consists of an elastic term and a dissipative one [13],

$$\mathbf{F}_\mathrm{n} = \min\left(0, -\rho\xi^{3/2} - \frac{3}{2}A_\mathrm{n}\rho\sqrt{\xi}\dot{\xi}\right)\mathbf{e}_\mathrm{n}, \qquad (1)$$

where the unit vector $\mathbf{e}_\mathrm{n}$ points towards the particle's center, and the "min()" function ensures that the force is always repulsive. In Eq. (1), ρ is defined as,

$$\rho = \frac{2Y\sqrt{R_\mathrm{eff}}}{3(1-\nu^2)}, \qquad (2)$$

where Y is the Young's modulus, ν is the Poisson's ratio and $R_\mathrm{eff} = R_1R_2/(R_1+R_2)$ is the so-called effective radius of the colliding particles (which have respective radii R_1 and R_2). Furthermore, the quantity A_n is the dissipative constant, which depends on elastic and viscous parameters of the particle's constituent material. The cor-

Powders and Grains 2013
AIP Conf. Proc. 1542, 185-188 (2013); doi: 10.1063/1.4811898

rect modeling of powder behaviour as a function of particle material requires accurately modeling A_n as a function of material parameters. While the dissipative constant is treated as an empiric parameter in most numerical studies, here we compute A_n using the analytical expressions for the normal coefficient of restitution derived in a recent theoretical study [15]. This study obtained accurate expressions for the coefficient of restitution (ε) associated with the normal collision between viscoelastic spheres as a function of material properties, A_n and the precollisional deformation rate (v_{imp}). Using these expressions and taking the value of ε which is associated with a given value of v_{imp} as obtained experimentally (see e.g. Refs. [16, 17, 18]), A_n can be calculated as a function of material properties and of the effective mass $m_{eff} = m_1 m_2/(m_1 + m_2)$, where m_1 and m_2 are the masses of the colliding particles [15].

Tangential forces — The tangential force reads [14],

$$\mathbf{F}_t = -\min\left[\mu|\mathbf{F}_n|, \int_{path} k_t\sqrt{R_{eff}\xi}\, ds + A_t\sqrt{R_{eff}\xi}\, v_t\right]\mathbf{e}_t, \quad (3)$$

where μ is the Coulomb friction coefficient and $k_t = 4G/(2-\nu)$ is the "stiffness" of the nonlinear spring associated with the elastic term of the tangential force, while the shear modulus, G, follows the equation $2G = Y/(1+\nu)$. The elastic term of the tangential force is calculated by integrating the force increments $\mathbf{dF} = k_t\sqrt{R_{eff}\xi}\,\mathbf{ds}$, which are associated with infinitesimally small tangential displacements $\mathbf{ds} = (\mathrm{d}s)\,\mathbf{e}_t$, over the total path covered by the particles during the contact [14]. Furthermore, the second term on the right-hand-side of Eq. (3) is the tangential damping force, with A_t and $\mathbf{v}_t = v_t\mathbf{e}_t$ standing for the tangential dissipative constant and relative tangential velocity, respectively [11]. The damping coefficient A_t is a parameter of the model, which must be determined from comparison of numerical simulations with experiments. We choose the value of A_t in such a manner that the prefactors which multiply the normal and tangential deformation rates ($\dot{\xi}$ and v_t) in Eqs. (1) and (3), respectively, have approximately the same order of magnitude, which gives $A_t \approx A_n Y/(1-\nu^2)$.

Multisphere method for modeling powder particles of complex geometric shapes

In order to model the complex geometric shape of powder particles used in additive manufacturing, we use the multisphere method, which consists of combining spheres of different sizes to build a rigid body [7, 19, 20, 21]. Spheres within a rigid body can overlap since they don't interact through any interparticle forces. The total force on the rigid body is computed by summing up the forces on all constituent spheres, whereas the resulting angular momentum of the complex particle is obtained from the total torque on all spheres with respect to the body's center of mass (see e.g. Ref. [19]).

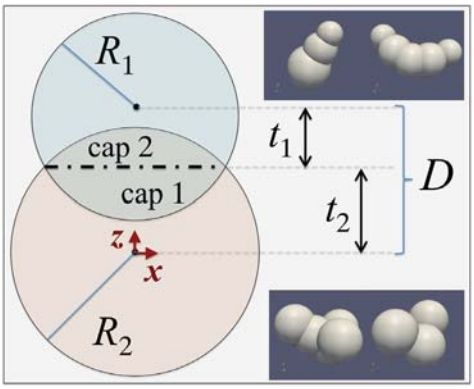

FIGURE 1. Schematic diagram of the overlap between two constituent spheres within a rigid body. D is the distance between the sphere's centers of radii R_1 and R_2, whereas t_1 and t_2 denote the distances from each sphere's center to its respective cap base. Some examples of particles constructed with the multisphere method in our simulations are shown as insets in the pictures in the upper and bottom right-hand corners.

However, one problem with the multisphere method concerns the calculation of the particle's moment of inertia [20, 21]. The overlap between spheres results in an excess (artifactual) contribution to the total moment of inertia of the rigid body, thus leading to incorrect prediction of its rotational behaviour. One solution for this problem is to compute the moment of inertia of each complex particle in the system numerically, e.g. using Monte Carlo [22]. Evidently, this alternative can become computationally too expensive if the system contains a large number of particles of different shapes. We compute the mass and the moment of inertia of each complex particle analytically, by explicitly removing the excess contribution due to the overlap volumes between constituent spheres. Our calculations are applicable when volume intersections of spheres in a rigid body involve not more than two spheres.

The amount of sphere-sphere overlap is defined by the distance D between the spheres' centers (cf Fig. 1). The contribution of the overlap to the total particle mass and moment of inertia of the rigid body is computed for all pairs of constituent spheres (labelled 1 and 2) for which $D < R_1 + R_2$. The mass $m_{overlap}$ of the overlap is the sum of the respective masses of caps 1 and 2, as depicted in Fig. 1. That is, $m_{overlap} = m_{cap\,1} + m_{cap\,2}$, where $m_{cap\,k} = [\rho_p\pi/3]\cdot\left[3R_k\ell_k^2 - \ell_k^3\right]$, with ρ_p standing for the material density, $\ell_k = R_k - t_k$ and $k = 1, 2$. Moreover, we compute the moment of inertia of the overlap volume by

considering, firstly, the case where the vector $\mathbf{D} = \mathbf{r}_1 - \mathbf{r}_2$ (where $\mathbf{r}_k$ stands for the center of mass position of sphere k) is parallel to the z axis (Fig. 1). In this manner, the moment of inertia tensor of each cap k ($\hat{\mathrm{I}}_{\mathrm{cap}\,k}$) is diagonal with components given by (see also Ref. [23] which uses the equations for DEM simulations of pharmaceutical tablets),

$$I_{xx,\mathrm{cap}\,k} = \frac{\rho_\mathrm{p}\pi}{4}\left[4R_k^3\ell_k^2 - \frac{16R_k^2\ell_k^3}{3} + 3R_k\ell_k^4 - \frac{3}{5}\ell_k^5\right] + \\ + m_{\mathrm{cap}\,k}\left[\left(L_{\mathrm{overlap}\,k} - L_{\mathrm{centroid}\,k}\right)^2 - L_{\mathrm{centroid}\,k}^2\right] = I_{yy,\mathrm{cap}\,k}, \quad (4)$$

$$I_{zz,\mathrm{cap}\,k} = \frac{\rho_\mathrm{p}\pi}{2}\left[\frac{4}{3}R_k^2\ell_k^3 - R_k\ell_k^4 + \frac{1}{5}\ell_k^5\right]. \quad (5)$$

In Eq. (4), $L_{\mathrm{centroid}\,k}$ is the geometric centroid of cap k, computed relative to the center of sphere k, while $L_{\mathrm{overlap}\,k}$ is the distance between the center of sphere k and the center of mass of the total overlap volume comprising caps 1 and 2. The tensor of inertia $\hat{\mathrm{I}}_{\mathrm{overlap},z}$ of the sphere-sphere intersection volume is then given by, $\hat{\mathrm{I}}_{\mathrm{overlap},z} = \hat{\mathrm{I}}_{\mathrm{cap}\,1} + \hat{\mathrm{I}}_{\mathrm{cap}\,2}$, whereas this equation considers that $\mathbf{D}$ is parallel to the z axis (Fig. 1). The tensor of inertia $\hat{\mathrm{I}}_{\mathrm{overlap}}$ for the case in which $\mathbf{D}$ makes an angle φ with the z axis reads, $\hat{\mathrm{I}}_{\mathrm{overlap}} = \hat{\mathrm{R}}\hat{\mathrm{I}}_{\mathrm{overlap},z}\hat{\mathrm{R}}^{-1}$, where $\hat{\mathrm{R}}$ is the rotation matrix associated with the rotation of a vector by an angle φ around the axis $\mathbf{e}_\mathrm{D} \times \mathbf{e}_\mathrm{z}$, with $\mathbf{e}_\mathrm{D} = \mathbf{D}/|\mathbf{D}|$.

Using the values of the mass m_{overlap} and tensor of inertia $\hat{\mathrm{I}}_{\mathrm{overlap}}$ of the sphere-sphere intersections within the rigid body, we then calculate the body's total mass m_{body}, center-of-mass position $\mathbf{r}_{\mathrm{cm}}$ and inertia tensor $\hat{\mathrm{I}}_{\mathrm{body}}$. The equations for m_{body} and $\mathbf{r}_{\mathrm{cm}}$ read,

$$m_{\mathrm{body}} = \sum_{i=1}^{N_\mathrm{s}} m_{\mathrm{sphere}\,i} - \sum_{j=1}^{N_\mathrm{o}} m_{\mathrm{overlap}\,j}, \quad (6)$$

$$\mathbf{r}_{\mathrm{cm}} = m_{\mathrm{body}}^{-1}\left[\sum_{i=1}^{N_\mathrm{s}} m_{\mathrm{sphere}\,i}\mathbf{r}_i - \sum_{j=1}^{N_\mathrm{o}} m_{\mathrm{overlap}\,j}\mathbf{r}_j\right], \quad (7)$$

where N_s (N_o) is the number of spheres (caps pairs) in the body, while $\mathbf{r}_{i(j)}$ denotes the center-of-mass position of sphere i (caps pair j). Furthermore, $\hat{\mathrm{I}}_{\mathrm{body}}$ reads,

$$\hat{\mathrm{I}}_{\mathrm{body}} = \sum_{i=1}^{N_\mathrm{s}} \frac{2}{5} m_{\mathrm{sphere}\,i} R_i^2\,\hat{1} - \sum_{j=1}^{N_\mathrm{o}} \hat{\mathrm{I}}_{\mathrm{overlap}\,j} + \hat{\mathrm{A}}, \quad (8)$$

where $\hat{\mathrm{A}}$ is the inertia tensor associated with a discrete distribution of mass elements m_k, each representing either a sphere or a pair of caps. That is,

$$\hat{\mathrm{A}} = \sum a_k m_k \begin{bmatrix} Y_k^2 + Z_k^2 & -X_kY_k & -X_kZ_k \\ -X_kY_k & X_k^2 + Z_k^2 & -Y_kZ_k \\ -X_kZ_k & -Y_kZ_k & X_k^2 + Y_k^2 \end{bmatrix}, \quad (9)$$

where $a_k = 1$ (-1) for spheres (caps pairs), while X_k, Y_k and Z_k are the distances between the center-of-mass of element k and the body's principal axes. The inertia tensor is then diagonalized by performing a principal axis transformation, whereas the normalized eigenvectors obtained from this transformation yield the orthogonal transformation matrix $\hat{J}$. Using this matrix, a vector $\vec{u}$ in the body's fixed frame of reference is transformed to the inertial frame through the equation, $\vec{u}_{\mathrm{in}} = \hat{J}\vec{u}$.

The motion of the rigid body is then computed by numerically solving the Newton's equation of motion, $m_{\mathrm{body}}\ddot{\mathbf{r}}_{\mathrm{cm}} = \sum_{i=1}^{N_\mathrm{s}} \mathbf{F}_i + m_{\mathrm{body}}\mathbf{g}$, where $\mathbf{g}$ is gravity and $\mathbf{F}_i$ is the total force on the i-th constituent sphere due to collisions with the device's walls or with particles belonging to other rigid bodies. Furthermore, the resultant torque $\mathbf{M}$ on the rigid body is given by, $\mathbf{M} = \sum_{i=1}^{N_\mathrm{s}} (\mathbf{r}_i - \mathbf{r}_{\mathrm{cm}}) \times \mathbf{F}_{\mathrm{t},i}$, where $\mathbf{F}_{\mathrm{t},i}$ is the tangential force on the body's i-th constituent sphere, while the angular velocity of the body, $\vec{\omega}$, evolves according to the Euler equations in the body's fixed frame, $\hat{I}\dot{\vec{\omega}} + \vec{\omega} \times (\hat{I}\vec{\omega}) = \hat{J}^{-1}\mathbf{M}$.

Modeling the boundary conditions for the powder particles

Our simulations must account for dynamic boundary conditions which are associated with the transport of the particles in the device's complex geometry. By using the DEM solver of Ref. [14], triangular meshes can be imported and interpreted as frictional walls for the granular material. In this manner, moving boundaries (walls) of nearly arbitrary geometric complexity can be modelled [14]. The forces acting on a particle of mass m_1 and radius R_1 upon collision with a wall of the experimental device are computed using the same model equations listed above with $m_{\mathrm{eff}} = m_1$ and $R_{\mathrm{eff}} = R_1$ (which means that, at the particle-wall contact point, the particle interacts with an effective "sphere" of infinite mass and radius) [14].

In Fig. 2 we show snapshots of a simulation of the transport of particles with complex shapes, built with the multisphere method, in a device which mimics the experimental apparatus [2]. The device consists of a rake for powder application (which moves from left to right in Fig. 2) and a building tank (central area). This building tank is filled with a powder layer which provides the base for the part to build, and is on top of a vertically adjustable platform. In the simulation of Fig. 2, frictional, vertical walls are placed at the borders of the device's platform. The simulation starts by releasing about 6500 particles from a small distance above the surface of the device's platform, as shown in Fig. 2a. After falling due to the action of gravity, particles are transported into the building tank as the rake moves from left to right (Fig. 2b-d). With the help of the simulations, several questions of relevance for the additive manufacturing process can be addressed, such as the role of particle

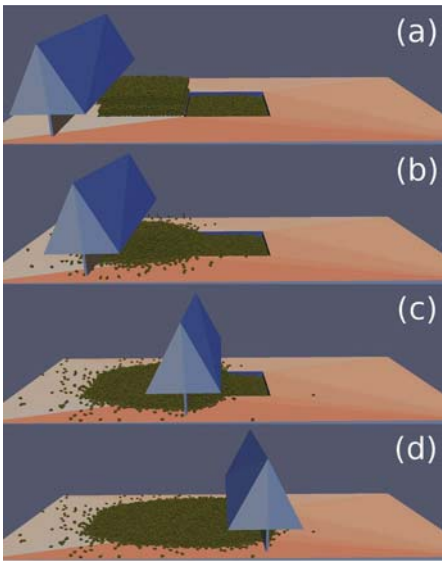

FIGURE 2. Snapshots of a simulation of particles with complex geometric shapes, built with the multisphere method, in dynamic boundary conditions which mimic the device used in additive manufacturing.

shape and size distribution for the flowability of the powder within the geometric device, center-of-mass position of the powder bed and surface profile of the granular material within the building tank.

CONCLUDING REMARKS

In conclusion, we develop a numerical tool for simulating the dynamic behaviour of powder particles of complex geometric shapes in additive manufacturing. Particles of complex shapes are built with the multisphere method, whereas the moment of inertia of sphere clumps is calculated analytically by excluding the additional (artifactual) contribution of sphere-sphere intersections to the particle's inertial properties. In the future, our model should be improved in order to account for cohesional forces, as well as for changes in mechanical properties of the particles due to the temperature fields and particle deformation. While the latter factor is negligible for metallic powders [2], it must be incorporated into our simulations in order to make them applicable for powders of thermoplastic materials [4, 5].

ACKNOWLEDGMENTS

We thank Thorsten Pöschel for review of an early version of the manuscript and Andreas Bauereiß and Aldo Glielmo for discussions. We acknowledge support from the German Research Foundation (DFG) within the frame of the Collaborative Research Initiative "Additive Manufacturing" (SFB 814) and through the Cluster of Excellence "Engineering of Advanced Materials".

REFERENCES

1. I. Campbell, D. Bourell and I. Gibson, *Rapid Prototyping J.* **18**, 255–258 (2012).
2. P. Heinl, A. Rottmair, C. Körner and R. F. Singer, *Adv. Eng. Mater.* **9**, 360–364 (2007).
3. K. P. Karunakaran, A. Bernard, S. Suryakumar, L. Dembinski and G. Taillandier, *Rapid Prototyping J.* **18**, 264–280 (2012).
4. B. Wendel, D. Rietzel, F. Kühnlein, R. Feulner, G. Hülder and E. Schmachtenberg, *Macromol. Mater. Eng.* **293**, 799–809 (2008).
5. R. D. Goodridge, C. J. Tuck and R. J. M. Hague, *Prog. Mater. Sci.* **57**, 229–267 (2012).
6. K. Abdel Ghany and S. F. Moustafa, *Rapid Prototyping J.* **12**, 86–94 (2006).
7. J. A. C. Gallas and S. Sokolowski, *Int. J. Mod. Phys.* **7**, 2037–2046 (1993).
8. T. Pöschel and V. Buchholtz, *Phys. Rev. Lett.* **71**, 3964–3966 (1993).
9. H. J. Herrmann, *Int. J. Mod. Phys. C* **4**, 309–316 (1993).
10. J. Schäfer, S. Dippel and D. E. Wolf, *J. Phys. I France* **6**, 5–20.
11. L. E. Silbert, D. Ertaş, G. S. Grest, T. C. Halsey, D. Levine and S. J. Plimpton, *Phys. Rev. E* **64**, 051302 (2001).
12. H. P. Zhang and H. A. Makse, *Phys. Rev. E* **72**, 011301 (2005).
13. T. Pöschel and T. Schwager. *Computational Granular Dynamics*, Springer, Heidelberg, 2005, 322 pp.
14. C. Kloss, C. Goniva, A. Hager, S. Amberger and S. Pirker, *Prog. Comput. Fluid Dy.* **12**, 140–152 (2012); `http://www.liggghts.com`.
15. P. Müller and T. Pöschel, *Phys. Rev. E* **84**, 021302 (2011).
16. Y. S. Cheong, M. J. Adams, M. J. Hounslow and A. D. Salman, *Chem. Eng. Res. Design* **83**, 1276–1282 (2005).
17. A. B. Stevens and C. M. Hrenya, *Powder Technol.* **154**, 99–109 (2005).
18. M. Montaine, M. Heckel, C. Krülle, T. Schwager and T. Pöschel, *Phys. Rev. E* **84** 041306 (2011).
19. H. Kruggel-Emden, S. Rickelt, S. Wirtz and V. Scherer, *Powder Technol.* **188**, 153-165 (2008).
20. X. Garcia, J. -P. Latham, J. Xiang and J. P. Harrison, *Géotechnique* **59**, 779–784 (2009).
21. J. F. Ferellec and G. R. McDowell, *Granular Matter* **12**, 459–467 (2010).
22. S. Amberger, M. Friedl, C. Goniva, S. Pirker and C. Kloss, "Approximation of objects by spheres for multisphere simulations in DEM", in *ECCOMAS-2012*, edited by J. Eberhardsteiner et al.
23. M. Kodam, J. Curtis, B. Hancock and C. Wassgren, *Chem. Eng. Sci.* **69**, 587–601 (2012).